https://doi.org/10.2352/ISSN.2169-4451.2021.37.32

Versatility of Laser Enhanced Direct Print Additive Manufacturing

Omer F. Firat[#1], Roger Tipton[2], Venkat Bhethanabotla[2], Jing Wang[3], and Thomas Weller[1]
[1] School of Electrical Engineering and Computer Science, Oregon State University, Corvallis, OR, USA
[2] Department of Chemical Biological and Materials Engineering, University of South Florida, Tampa, FL, USA
[3] Department of Electrical Engineering, University of South Florida, Tampa, FL, USA
[#]firato@oregonstate.edu

Abstract

This paper provides examples of the use of direct print additive manufacturing to fabricate RF/microwave and optical components. Direct print additive manufacturing is the combination of extrusion and micro-dispensing on a single tool. The design, 3D printing process and material selections for finite ground coplanar waveguide (FG-CPW) planar transmission lines, the integration of DC contact RF MEMS switches within the FG-CPWs, and optical interconnects are detailed. Picosecond-pulsed laser machining is performed to enhance the finish quality of the devices and achieve minimum feature size down to 6 µm specifically for the RF switch.

Introduction

Interest in using additive manufacturing (AM) techniques has been steadily growing in recent years. Important advances have expanded AM processing capabilities, including the commercially available variety of printable materials and achievable minimum feature size. In addition, the wide-spectrum application of AM in diverse applications such as aerospace, biomedical as well as RF and microwave technologies has increased. For example, next generation jet engine fuel nozzles will be 3D printed, yielding an improvement of approximately 10% fuel efficiency [1]. Printed electronics, a focus of this paper, has a market value of $7.8 billion in 2020 with projected growth at a compound annual growth rate (CAGR) of 21.5% from 2020 to 2025. By considering the emergence and demand of 5G and related millimeter-wave packaging technology, this growth is projected to increase at a greater rate.

Direct print additive manufacturing (DPAM) is a fabrication method that is capable of printing multi-material 3D structures in a single platform [2–4]. DPAM combines fused deposition modeling (FDM) for thermoplastics and microdispensing for inks and pastes. Laser enhanced direct printed additive manufacturing (LE-DPAM), the combination of laser processing with DPAM, is a shape deposition manufacturing (SDM) process where complex parts are made by combining material additive and subtractive processes in the same piece of automation. In the case of the nScrypt 3D printer used in this work, FDM enables not only thermoplastic printing, but also thermoplastic-ceramic high-K materials and optical fibers with extruding temperature up to 450°C. FDM also has a great design flexibility with a capability of large z dimensional fabrication. For example, FDM can extrude from the minimum layer thickness of 14 µm [5] to as thick as required for structures, whereas microdispensing is capable of printing down to a 25 µm thickness of conductive layers on a substrate with a minimum feature size of 100 µm [6]. With microdispensing, it is possible to print a variety of pastes including conductive, resistive, and PZT slurry with a viscosity range from 1 to 10^6 cP. A single platform with a high precision positioning system, used for FDM and microdispensing, is utilized to cure conductive pastes at the desired temperature, so

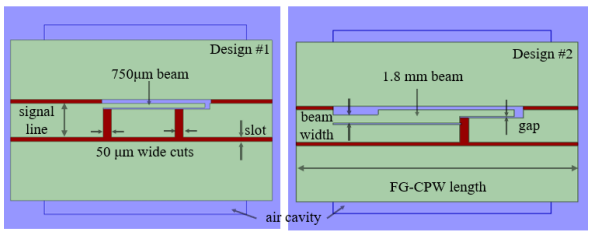

(a) (b)

Fig. 1. RF MEMS switch designs in suspended FG-CPW, (a) design #1, and (b) design #2. Purple, brown and green represent ABS substrate, ABS suspended bridge and CB028, respectively.

DPAM can enable the printing of a complete multi material device with a high precision.

One of the most important advantages of AM is to realize relatively complex geometrical structures with minimal infrastructure that generates low material waste. In the case of RF and microwave circuits, traditional fabrication processes require multiple steps, including photolithography and etching, while AM methods include print and cure processes in a cost-effective manner without requiring toxic materials such as photoresist developer and chemical etchants. In this sense, AM offers a possible alternative technology that can displace conventional fabrication techniques such as molding, milling, PCB, and photolithography.

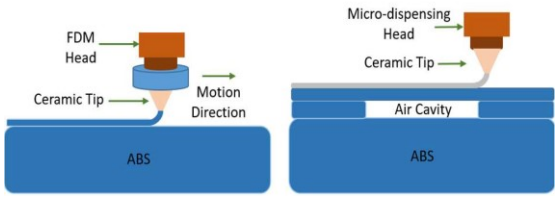

(a) (b)

Fig. 2 (a) Case #1; Direct print additive manufacturing (DPAM) process for (a) FDM to deposit ABS substrate with the embedded cavity; (b) CB028 micro- dispensing on top of printed ABS bridge suspended across the cavity.

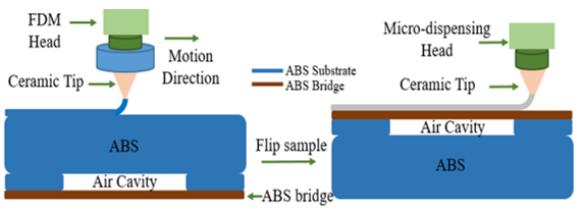

(a) (b)

Fig. 2 (b). Case #2: (a) FDM; (b) micro dispensing

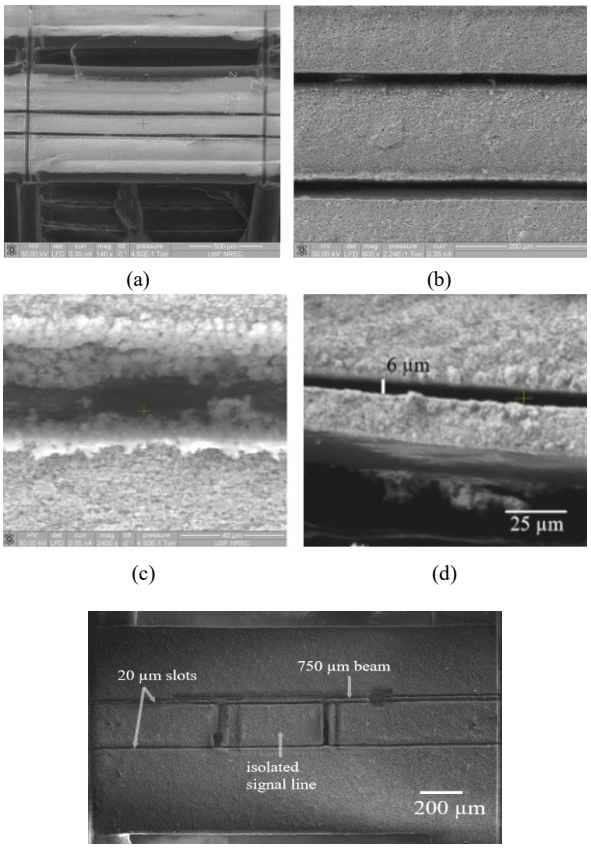

Fig. 3. SEM images of (a-b) laser machined AM CPW crossovers; (c) 20 µm slot in silver paste; (d) the sidewall of the cantilever beam; (e) RF switch cantilever beam design #1 incorporated within the CPW signal line.

LE-DPAM has the potential to enable low parasitic and tight integration of high-performance packaging systems with integrated circuits. Several 3D printed optical and RF components and circuits such as transmission lines, on-chip passives, multilayer packages, interconnects, antennas, waveguides, and filters have been successfully demonstrated with low cost and comparable performance with other traditional fabrication techniques [7-9].

In this paper, the feasibility of AM with the realization of LE-DPAM electrical, electromechanical, and optical applications is presented. The fabrication processes are detailed by showing the capability of controlling surface roughness, aspect ratio, layer thickness, that influences RF and optical performance of the fabricated devices.

Electrical and Electromechanical Applications

One example of an electrical application of LE-DPAM is a new type of versatile 3D printed suspended finite ground coplanar waveguide (FG-CPW) interconnect for mm-wave packaging systems. This new approach of suspended interconnects can be utilized into an integrated system with the System-on-Package (SoP) method at microwave and mm-wave frequencies. Direct integration of multiple passive and active components with fairly low coupling can be utilized with the new suspended CPWs. They are patterned on a fixed-fixed beam and can be extended over an air cavity to other components as detailed in [10].

A new type of 3D printed electrostatically actuated radio frequency microelectromechanical systems (RF MEMS) switch

Table 1. FG-CPW and switch dimensions

	FG-CPW			Switch		
Design No	Length (µm)	Signal width (µm)	Slot (µm)	Length (µm)	Width (µm)	Gap (µm)
#1	1500	180	20	750	20	6
#2	2400	180	20	1800	40	7

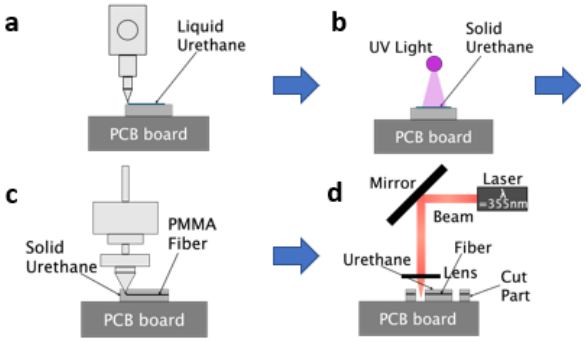

Fig. 4. Using a composite additive and subtractive LE-DPAM process for producing CCS optical fiber interconnects on a PCB board. (a) The LE-DPAM printing process for fabricating an optical interconnect where an FDM additive manufacturing tool is used to print an ABS base on a PCB board to get the fibers to the correct end facet heights to align components and a cladding material is micro-dispensed onto the substrate. (b) The cladding material is cured with UV energy. (c) The fiber is embedded within the cladding material. (d) The end facets are prepared using a subtractive laser process, and finally components are mounted to the board where communication is via the CCS optical fiber interconnect.

that is integrated within the suspended FG-CPW is demonstrated for the electromechanical aspect of LE-DPAM (Fig 1). RF MEMS switches are important components for RF circuits and are utilized in wireless communications and defense applications, etc. There are two important parameters for electrostatic RF switches, the RF performance and the actuation or pull-in voltage. The switch is in the form of a cantilever fixed-free beam and is laser machined within the signal trace of the suspended CPWs as detailed in [12].

AM has advantages over traditional RF switch techniques such as compatibility with package integration, material variety with lower elasticity, which directly affects pull-in voltage, and low cost. For example, widely used MEMS structural materials, Si, Ni, and Ag have a Young's modulus of 160 GPa, 77.5 GPa, and 207 GPa, respectively, while ABS and Dupont CB028, two widely used 3D printable materials, have much lower Young's modulus of 1.57 GPa and 7.71 GPa, respectively.

Design and Fabrication Flow of Suspended CPW and Cantilever Beam

ABS is a thermoplastic material with a measured dielectric constant (ε_r) of 2.35 and a loss tangent ($\tan\delta$) of 0.0065 at 30 GHz [11] and is printed with an FDM process. ABS is extruded with 125 µm inner / 175 µm outer diameter ceramic nozzle at 235°C onto a 110°C heated metal printer platform to form the substrate (nScrypt 3Dn tabletop).

Since the device is essentially suspended and needs a suspended layer, a form of cavity is required underneath the top ABS layer (suspended ABS bridge) and there are two ways to achieve this. First (case #1), a suspended ABS bridge could be printed as a top layer as seen in Fig. 2 (a). Extrusion of ABS filaments through a ceramic tip ends up as a cylindrical shape and

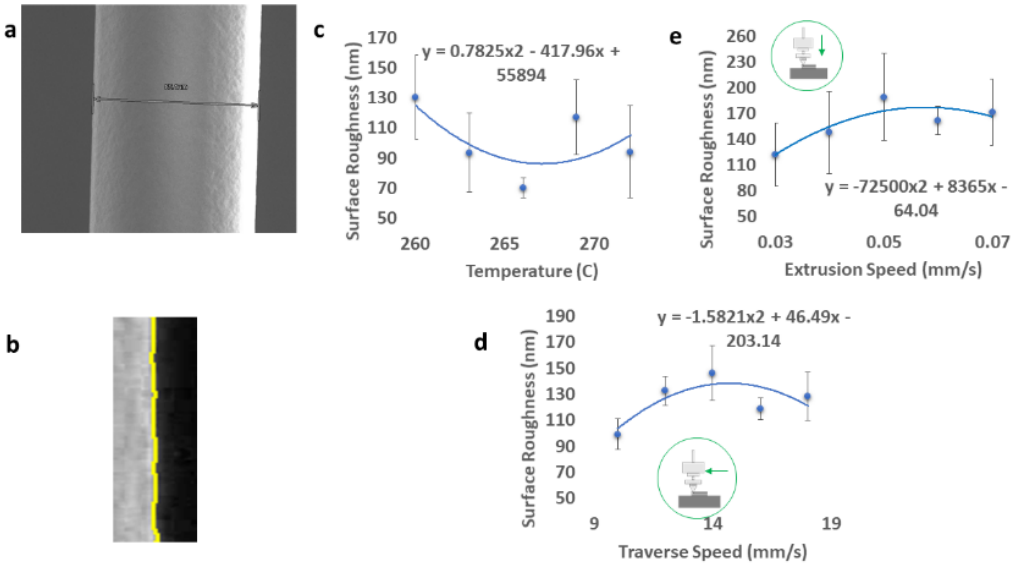

Fig. 5. Optimization of key processing parameters yields a surface roughness of less than 100 nm for a 70-µm fiber. (a) SEM image of the surface roughness of a 70-µm PMMA fiber from a 50-µm zirconia nozzle. (b) Using an image processing software, ImageJ Fuji macro Analyze_Stripes, to determine average surface roughness from SEM images. (c) Effect of temperature on surface roughness with about 266°C being the optimal nozzle temperature. (d) Effect of traverse speed on surface roughness showing slower traverse speeds resulting in smaller surface roughness. (e) Effect of Filament Feed Speed on surface roughness showing slower feed speeds resulting in smaller surface roughness.

the thick ABS bridges over the air cavity. A single suspended ABS bridge diameter is the outer diameter of the ceramic nozzle (for this case, 175 µm). Second (case #2), the suspended top ABS layer could be printed as a first layer in the substrate and by flipping it over, the suspended layer could be the top layer as seen in Fig. 2 (b). The thickness and shape of this layer, that becomes the suspended ABS bridge by flipping the structure, can be controlled easily because it prints directly over the printer bed.

Since surface roughness is an important parameter for especially high frequency RF applications due to the skin depth effect, the surface finish of the suspended ABS bridges needs to be smooth so that the conductive layer surface roughness would be smooth as well. Therefore, the case #2 fabrication procedure allows us to build devices with better RF performance.

After the design is completed, a 0.4 mm thick ABS substrate with 0.15 mm deep air cavity is formed along with printing 4 mm long suspended ABS bridges. For case #1, the thickness of the ABS bridges is approximately 175 µm while for case #2, it is around 50 µm. Laser heating can be applied to partially flatten the surface and reduce the thickness of the ABS bridges for case #1; thinning down to 125 µm is detailed in [10].

After the FDM print is performed, Dupont CB028 as a conductive paste is microdispensed using 125 µm inner / 175 µm outer diameter ceramic tip onto the suspended bridges to realize conductive traces with an average thickness of 30 µm. The printed samples are then cured in-situ at 90 °C for 1 hour to achieve 2e6 S/m conductivity [11].

Finally, laser machining is performed with a picosecond pulse laser to form 50-ohm CPW lines by machining 20 µm wide slots as seen in Fig 3 a-d. Average power (P_{avg}) of 0.4 W at a repetition rate of 100 KHz with a wavelength of 355 nm was used for the laser machining process. Laser machining enhances 3D printing finish quality due to the cold ablation effects and enables controlling the minimum dimensions of the critical features such as transducer gap of the RF switch cantilever beam down to a few microns with a high aspect ratio as seen in Fig. 3 (d). Laser machining needs to be perpendicular with the surface and precise focusing is essential to achieve high aspect ratio and to avoid any burning effect on materials. Also, CBO28 conductivity achieves 10e7 S/m [11] with the effect of cold ablation so the RF performance of CPW lines improves. Two designs of cantilever beams (Fig. 1) within the RF signal path of the suspended CPWs are laser machined to realize a RF MEMS switch (Fig 3-e) as detailed by Firat et al. [12], and their design dimensions are listed in Table 1.

Optical Application

New additive and subtractive manufacturing techniques have enabled the development of a new generation of optical fiber interconnect devices on rigid, including PCB boards, and flexible substrates. The basic process has been outlined by Tipton et al [5]. A 125 µm Kapton material is used as the substrate. A commercially UV-curable optical adhesive blend of aliphatic urethane acrylate and acrylate monomer (Norland 1369 optical adhesive) cladding material was added using an LDM process and partially cured using UV energy (BLAK-Ray Long Wave Ultraviolet Lamp, Model B 100 AP/R) under a nitrogen environment. A commercially available PMMA filament material (Treed, part number HIRMA) was used to extrude a 75 µm fiber is embedded into the middle of the cladding material using an additive FDM process. The new fiber/cladding assembly is fully cured. Finally, the end facets are prepared with the subtractive 355 nm picosecond laser [13]. The process and equipment are illustrated in Figure 4. Finished fiber optic interconnect assemblies have been produced up to 250 µm thick, 3 mm wide and 10 cm long.

Fiber Diameter and Temperature vs Surface Roughness

A low surface roughness is critical to the performance of an optical fiber interconnect. Commercial optical fibers have an RMS surface roughness of about 300 nm for a 62.5 µm fiber. A surface roughness of less than 100 nanometers has been achieved using the LE-DPAM process for a 75 µm optical fiber. FDM

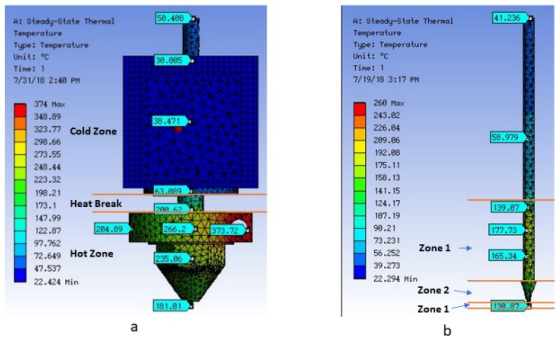

Fig. 6. Internal thermal profile of liquefier and PMMA material inside of the liquefier. (a) Steady state thermal analysis of the liquefier indicating temperature variation across liquefier. (b) Temperature variation of the PMMA melt within the liquefier indicating an entry temperature of 41°C at entry to 178°C at the heat break zone to 130°C at nozzle exit.

process is currently limited to fibers greater than 40 µm. New liquefier designs will be required to produce single mode fibers below 10 microns. The end facets need to be prepared using the laser and a wavelength of 193 nm is the optimum for PMMA fiber.

In the evaluation of the fiber surface roughness, low pressure SEM (Quanta 3D Dual Beam Imaging System) was used due to the nonconductive nature of the PMMA material and the small feature size of the surface variation (see Fig 5a). The RMS surface roughness was then characterized using image processing software from ImageJ, which was used to determine the edge of the fiber and then measured to determine the variation and the edge profile as shown in Fig 5b.

Surface roughness is dependent on processing conditions and nozzle diameter. The main processing variables in our FDM process are liquefier temperature, extruder filament speed, and extruder traverse speed. Through a design of experiments an optimum condition of 266ºC, 0.03 mm/s, and 10 mm/s respectively have produced an RMS surface roughness of about 80 nm for the 75 µm fiber as shown in Figure 5c, e, and d.

Fiber diameter also plays an important role in surface roughness. Below a diameter of about 40 µm extrusion forces increase in the liquefier. Below 40 µm, the surface roughness increases rapidly to over 600 nm for 14 µm fibers. This behavior can be quantitatively explained by the reduction in nozzle diameter increasing the force required to extrude the fiber. The force inside the liquefier is a function of the geometry, material properties, and the temperature inside the liquefier which effect the shear rate and pressure drop. Because of these changes in shear rate and pressure drop, the fiber surface roughness is affected, which in turn affects the transmission capabilities of the fiber.

The temperature distribution is the only unknown and must be measured internally or calculated using numerical simulation. For this study, the external temperatures were measured in six locations and ANSYS. Steady State Thermal was used to determine the internal temperature of the liquefier and the polymer melt. Our liquefier consists of a hot zone that is generated by a single rod type cartridge heater, a heat break zone, and a cooling zone, as indicated in Figure 6a. The purpose of these three different zones is to heat the PMMA material but prevent the heat from rising up the liquefier and melting the material before it is fully captured in the nozzle within the hot zone. Results of the numerical simulation for the polymer melt material are presented in Figure 6b. These internal temperatures are then used to solve for the pressure drop as presented by Bellini [14]

For a 1.75 mm filament diameter, the surface roughness as a function of the nozzle diameter x is described by the following equation [15]:

$$Surface\ Roughness \propto x^{-1.136} \qquad (1)$$

A reduction in filament diameter from 1.75 to 1.0 mm is one possible way of improving the surface roughness in smaller diameter fibers.

Conclusion

The versatility of laser enhanced direct print additive manufacturing is demonstrated with its applications in three main categories, namely electrical, electromechanical, and optical. LE-DPAM enables interconnects for mm-wave integrated packaging, RF MEMS switches and optical interconnects. The fabrication steps with optimization processes are detailed along with the demonstration of a variety of printable materials.

References

[1] Jet engine WITH 3D-Printed Parts Powers Next-Gen Boeing 737 max for the first time. GE News. (n.d.). https://www.ge.com/news/reports/jet-engine-with-3d-printed-parts-powers-next-gen-boeing-737-max-for-the-first-time.

[2] Weiss, L., and F. Prinz. “Novel Applications and Implementations of Shape Deposition Manufacturing.” (1998).

[3] Williams, Christopher & Mistree, Farrokh & Rosen, David. A Functional Classification Framework for the Conceptual Design of Layered Manufacturing Technologies. Journal of Mechanical Design. 133. 10.1115/DETC2008-49353. (2008)

[4] Perez, K. B., and Christopher B. Williams. “Combining Additive Manufacturing and Direct Write for Integrated Electronics.” (2013).

[5] R.B. Tipton, D. Hou, E.A. Rojas-Nastrucci, T.M. Weller, V.R. Bhethanabotla, “Laser Enhanced Direct Print Additive Manufacturing of Embedded Circular Cross-Section Optical Fiber Interconnects for Board Level Computing Devices”, Additive Manufacturing. 34 (2020).

[6] E. A. Rojas-Nastrucci, A. D. Snider, and T. M. Weller, ″Propagation Characteristics and Modeling of Meshed Ground Coplanar Waveguide,″ IEEE Transactions on Microwave Theory and Techniques, vol. 64, pp. 3460-3468, (2016).

[7] D. Hawatmeh and T. Weller, "2.4 GHz Band Pass Filter Architecture for Direct Print Additive Manufacturing," 2018 IEEE/MTT-S International Microwave Symposium - IMS, Philadelphia, PA, pp. 67-70. (2018).

[8] C. Mariotti, F. Alimenti, L. Roselli and M. M. Tentzeris, "High-Performance RF Devices and Components on Flexible Cellulose Substrate by Vertically Integrated Additive Manufacturing Technologies," in IEEE Transactions on Microwave Theory and Techniques, vol. 65, no. 1, pp. 62-71. (2017)

[9] R. A. Ramirez, D. Lan, J. Wang and T. M. Weller, "MMIC packaging and on-chip low-loss lateral interconnection using additive manufacturing and laser machining,″ 2017 IEEE MTT-S International Microwave Symposium (IMS), Honolulu, HI, pp. 38-40. (2017).

[10] O. F. Firat, M. Abdin, J. Wang and T. M. Weller, "Low-loss suspended crossover interconnects using laser enhanced direct print additive manufacturing," 2019 IEEE 20th Wireless and Microwave Technology Conference (WAMICON), Cocoa Beach, FL, USA, pp. 1-4. (2019).

[11] E. A. Rojas-Nastrucci et al., "Characterization and Modeling of K-Band Coplanar Waveguides Digitally Manufactured Using Pulsed Picosecond Laser Machining of Thick-Film Conductive Paste," in IEEE Transactions on Microwave Theory and Techniques, vol. 65, no. 9, pp. 3180-3187. (2017).

[12] Omer Firat, J. Wang, and T. Weller, “Additively Manufactured, Low Loss 20 GHz DC Contact RF MEMS Switch Using Laterally

Actuated, Fix-Free Beam, “Accepted to the 2021 IEEE MTT-S International Microwave Symposium (IMS) (2021).
[13] D. Hou, “Additive Manufactured and Laser Enhanced Optical Fiber on Flexible Kapton Substrate”, Graduate Theses and Dissertations. https://scholarcommons.usf.edu/etd/8226. (2020).
[14] A. Bellini, S. Guceri, M. Bertoldi, S. Güçeri, M. Bertoldi, “Liquefier Dynamics in Fused Deposition”, Journal of Manufacturing Science and Engineering. 126, 237–246. (2004).
[15] V.B. RB Tipton, D Hou, TM Weller, “Direct Print Additive Manufacturing of Optical Fiber Interconnects for Board Level Computing Devices”, 2019 AIChE Annual Meeting. (2019).

Author Biography

Omer Firat received his BS in electrical engineering from Inonu University, Turkey (2013) and his master’s in electrical and computer engineering from University of Delaware (2017) and, currently pursues his Ph. D in electrical engineering at Oregon State University. His research interests; RF switches and reconfigurable additively manufactured RF circuits.

Roger B. Tipton is a PhD Candidate in the Department of Chemical, Biological, and Materials Engineering at University of South Florida. His research interests include additive manufacturing, flexible optical and electronic sensors, and sensor applications for industry to improve user performance, health, and safety.

Venkat Bhethanabotla obtained his B.S. from Osmania University in Hyderabad, India, and Ph.D. from Penn State in PA, USA, both in Chemical Engineering. He is a Professor of Chemical & Biomedical Engineering and Director of the Materials Science and Engineering Program at University of South Florida.

Jing Wang received two B.S. from and M.S. degrees from Tsinghua University, China (1994) and University of Michigan, in both electrical engineering (2000), and mechanical engineering (2002), and Ph.D. from University of Michigan (2006). He is currently a professor in Electrical Engineering at University of South Florida.

Thomas Weller received the B.S., M.S., and Ph.D. degrees in Electrical Engineering in 1988, 1991, and 1995, respectively, from University of Michigan. He was a faculty member at University of South Florida (1995-2018). He joined Oregon State University in 2018 and is the Gaulke Professor and School Head in Electrical Engineering and Computer Science.